electronics

MDPI

Article

Empirical Performance Evaluation of 5G Millimeter Wave System for Industrial-Use Cases in Real Production Environment

Jordi Biosca Caro [1,*], Junaid Ansari [1], Bengt-Erik Olsson [2], Niklas Beckmann [3], Niels König [3], Robert H. Schmitt [3], Falko Popp [4] and Daniel Scheike-Momberg [4]

[1] Ericsson, Ericsson Allee 1, 52314 Herzogenrath, Germany; junaid.ansari@ericsson.com
[2] Ericsson, Lindholmspiren 11, 417 56 Göteborg, Sweden; bengt-erik.olsson@ericsson.com
[3] Fraunhofer Institute for Production Technology (IPT), Steinbacherstr. 17, 52074 Aachen, Germany; niklas.beckmann@ipt.fraunhofer.de (N.B.); niels.koenig@ipt.fraunhofer.de (N.K.); robert.schmitt@ipt.fraunhofer.de (R.H.S.)
[4] Qualcomm, Nordostpark 89, 90411 Nuremberg, Germany; fpopp@qti.qualcomm.com (F.P.); dscheike@qti.qualcomm.com (D.S.-M.)
* Correspondence: jordi.biosca.caro@ericsson.com

Abstract: Wireless communication plays an important role in the digitization of industries. A 5G cellular communication system enables several industrial automation use cases. Fifth-generation deployments in industrial use cases have mainly been carried out in the sub-7 GHz frequency range. In this work, we empirically study 5G system performance in the millimeter wavelength (mmW) range for industrial use cases: additive manufacturing processes and precision manufacturing robotics. We carry out an experimental performance evaluation of a commercially available non-public 5G mmW system to assess its latency, reliability and throughput for uplink and downlink data traffic in a real industrial environment. We also investigate the impact of various 5G configurations on 5G performance characteristics with insights from the baseband log information as well as unidirectional latency measurements. Our empirical results indicate that 5G mmW system can achieve low latency with high reliability in both one-way traffic directions. The throughput is observed to be high for line-of-sight (LOS) scenarios, making the use of the 5G mmW system appealing especially for data rate-intensive and time-critical industrial use cases. We also observe that industrial environments with lots of metal and reflective surfaces provide favorable propagation conditions for non-LOS transmissions. Our results indicate that static industrial use cases with low mobility can leverage the performance benefits of 5G mmW systems.

Keywords: 5G non-public network; mmW; industrial deployment; additive manufacturing processes; precision manufacturing; mobile robotics; experimental performance evaluation; over-the-air performance testing

check for updates

Academic Editor: Christos J. Bouras

Received: 20 December 2024
Revised: 21 January 2025
Accepted: 27 January 2025
Published: 4 February 2025

Citation: Biosca Caro, J.; Ansari, J.; Olsson, B.-E.; Beckmann, N.; König, N.; Schmitt, R.H.; Popp, F.; Scheike-Momberg, D. Empirical Performance Evaluation of 5G Millimeter Wave System for Industrial-Use Cases in Real Production Environment. *Electronics* **2025**, *14*, 607. https://doi.org/10.3390/electronics14030607

Copyright: © 2025 by the authors. Licensee MDPI, Basel, Switzerland. This article is an open access article distributed under the terms and conditions of the Creative Commons Attribution (CC BY) license (https://creativecommons.org/licenses/by/4.0/).

1. Introduction

Wireless communication is expected to play a key role in enabling smart and flexible manufacturing and satisfy the reliable real-time communication requirements of industrial applications [1]. A 5G communication system is designed to address the communication demands of industrial applications in a scalable manner [2,3]. In contrast to other wireless technologies operating in shared frequencies, the use of dedicated frequencies by 5G circumvents wireless channel disturbances and interferences from other devices and networks. A dedicated spectrum also allows fast channel access without needing to

follow spectrum-sharing regulations such as duty cycle constraints, low transmit power limitations and the listen-before-talk procedure [4].

Fifth-generation operation in mmW frequencies (also known as Frequency Range 2 (FR2), which spans from 24.250 GHz to 52.600 GHz) offers unprecedented cellular bandwidth with potentially very low latency, making it of particular interest for industrial applications [5,6]. Naturally, propagation is more challenging in an mmW range compared to lower frequencies with higher penetration losses and less efficient diffraction characteristics. However, in industrial environments with lots of metal, moving machine parts, workers, etc., a large amount of reflected power into the non-line of sight (NLOS) can positively impact the coverage of the 5G mmW signal. A higher penetration loss in walls and building materials also allows for a good level of isolation between cells, for instance, in different factory halls, thereby reducing interference and improving performance. In this work, we experimentally evaluate the performance of 5G operation in mmW frequencies in a real production environment. We investigate industrial additive manufacturing processes and precision manufacturing robotic use cases based on the 5G mmW system at the Fraunhofer Institute for Production Technology (IPT) in Aachen, Germany. These use cases demand reliable low-latency communication with high demands on throughput, thereby making 5G mmW technology a well-suited candidate. The empirical investigation includes 5G deployment with line-of-sight (LOS), NLOS and obstructed-line-of-sight (OLOS) deployment scenarios. In particular, we measure the end-to-end one-way communication delay for the application traffic of the selected use cases, i.e., separate uplink and downlink latency behavior while considering the reliability aspects. In this context, the reliability of network layer packet transmissions is the percentage value of the packets successfully delivered to a given system entity within the time constraint required by the targeted service out of all the packets transmitted [7]. As an example from a mobile robotics application, 10 ms of communication latency (one-way) with successful packet delivery is to be guaranteed 99.9% of the time [8].

The rest of the article is organized as follows: Section 2 describes the related work on the use of the 5G mmW system in industrial deployments and performance characterization. Section 3 describes the industrial use cases and their requirements that were investigated on the shopfloor of the Fraunhofer Institute for Production Technology (IPT) [9]. Section 4 describes in detail our experimental methodology and measurement setup used to carry out a performance evaluation of the 5G mmW system for the investigated industrial use cases. Section 5 presents the empirical performance evaluation results and their analysis. Finally, the article is concluded, and future work directions are outlined in Section 6.

2. Related Work

Many industrial automation applications require highly reliable low-latency communication involving sensors, robots, machines, controllers, etc. [10,11]. Cloud-based architecture is becoming highly popular in industrial automation as it allows for flexibility, adaptability and the use of advanced analytics and decision making—often assisted by machine learning and artificial intelligence methods [12]. The communication patterns in industrial automation applications involve both uplink direction, for instance, from sensors to cloud-based controllers and decision-making entities, as well as in the downlink direction from the cloud to actuators such as robots and machines. The uplink and downlink traffic profiles are generally independent and different from each other in industrial applications [11]. Moreover, the one-way traffic performance of a 5G system is different due to different protocol signaling, communication and computational capabilities at the UEs and base stations, etc. Thus, simple round-trip-timing measurements (e.g., using the ICMP ping tool) do not give insights into the actual industrial automation application behavior.

Earlier 5G non-public-network (NPN) experimental evaluation studies in industrial deployments are conducted in the sub-7 GHz frequencies [13,14]. While the design principles of the 5G system and many technical features remain the same, there are significant differences in the propagation characteristics, the available bandwidth, and the spectrum regulations in the mmW frequency range compared to sub-7 GHz. This led to operational differences and a different selection of parameters such as the beam management operation, orthogonal frequency-division duplexing (OFDM) sub-carrier spacings, etc., for 5G mmW operation, directly impacting the key performance indicators (KPIs). Several industrial use cases demand high uplink capacity [15]. As a result, the available bandwidth in the sub-7 GHz frequency range is becoming increasingly constrained for several industrial automation applications. While the third-generation partnership project (3GPP) specified schemes such as multi-user multiple-input, multiple-output (MU-MIMO), small cells and handover mechanisms to mitigate the bandwidth constraints, albeit with additional signaling and processing overhead, mmW frequencies, especially the 26 GHz frequency range, offer a large bandwidth, which becomes attractive for industrial applications requiring high data rates.

mmW communication has been intensively investigated using simulations and mathematical analysis [16–18]. The past experimental performance characterization of mmW communication primarily aims for high data rate applications [19–22]. To the best of our knowledge, a comprehensive experimental evaluation study of 5G mmW system in terms of reliable low-latency communication in a real industrial environment has not been reported.

Nonetheless, Zheng et al. have carried out an early experimental validation of the large capacity gains of a commercial 5G mmW system in both indoor and outdoor deployment scenarios [23]. The authors investigate the penetration loss in indoor and outdoor scenarios with various obstructing objects such as glass, humans, etc., and its comparative performance aspects in terms of throughput degradation and increase in the roundtrip time measurements. Their findings indicate that 5G mmW transmissions show a noticeable performance loss with obstruction and the increasing distance between the transmitting and receiving antennas.

It is argued that mmW systems may not be suitable for latency-critical industrial communication owing to their vulnerability to penetration losses and blockage [24]. Danger et al. have shown in their empirical study, conducted in a real production environment using commercially available 5G mmW equipment, that acceptable downlink and uplink throughput can be achieved with LOS and NLOS propagation scenarios [25], but they have not conducted latency analysis. In comparison to the earlier findings by Zheng et al., industrial environments provide better propagation for mmW transmissions due to higher reflections, unlike other indoor environments. Danger et al. demonstrate that the careful placement of passive reflective surfaces can help reach the receiving antennas effectively beyond LOS deployment scenarios [25]. Other studies [26] also show that Intelligent Reflective Surfaces (IRSs) help in NLOS and beyond the LOS propagation of directional transmissions.

Ayadurai et al. conducted a study on the feasibility of a closed-loop industrial control scenario using a 5G mmW system [27]. In contrast to the common belief that mmW transmissions suffer from high degrees of blockage and propagation losses, Ayadurai et al. observe that multipath reflections and the beam (re-)selection scheme of 5G systems can provide sufficiently good NLOS propagation in industrial deployments.

3. Smart Manufacturing and Mobile Robotic Use Cases

In this section, we describe two use cases investigated in this work on the Fraunhofer IPT shopfloor: (1) the usage of a thermal camera for additive manufacturing processes and (2) the use of mobile robots for manufacturing automation.

3.1. Additive Manufacturing Processes

Additive manufacturing processes are a set of technologies that create three-dimensional objects by sequentially adding materials layer by layer from digital models, enabling complex geometries, customization and material efficiency [28]. Fraunhofer IPT has developed the Multi-Technology Robot System for Adaptive Manufacturing (MIRA), combining multiple manufacturing technologies in one robot cell [29]. In this regard, an additive manufacturing process classified as Directed Energy Deposition is introduced. The process consists of a laser beam melting a metallic wire as it is laid onto a substrate. This technique is known as Laser Metal Deposition with wire (LMD-w) [30]. In this process, a metal alloy wire is typically fed into the laser beam at a specified position. The heat from the high-power laser efficiently melts the wire, forming a melted pool between the wire and the substrate plate. This ongoing supply of wire material into the melted pool allows for precise deposition onto the target surface. For this use case, the function of a thermal camera is essential for the real-time monitoring of the temperature distribution, thereby supporting both quality assurance and process optimization. The thermal camera, VarioCAM HD head 800, as shown in Figure 1, generates high-resolution thermal images.

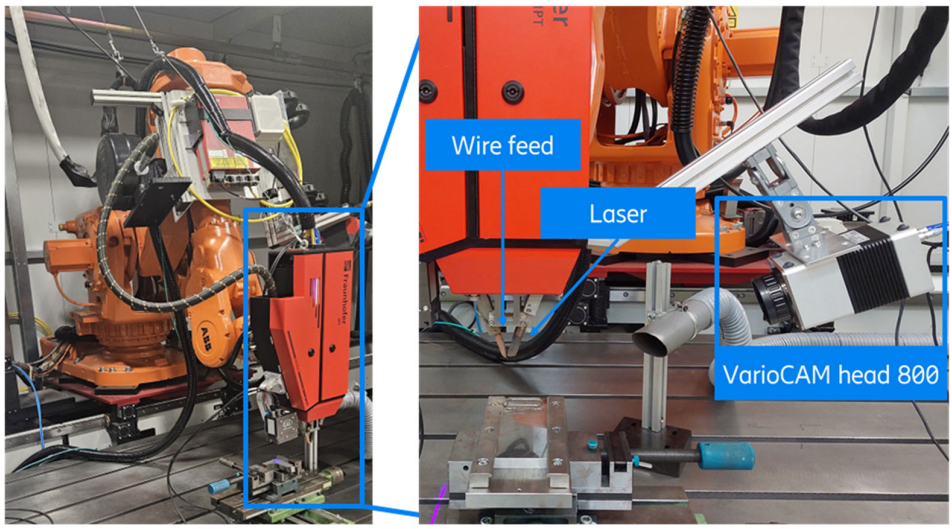


Figure 1. Snapshots of the additive manufacturing process using Laser Metal Deposition with wire.

The camera data stream from VarioCAM HD head 800 needs to be transmitted to a data-processing unit in the (edge) cloud for the real-time monitoring and control of the laser beam and wire feeding mechanism, which is illustrated in Figure 2. The transmission of the images effectively requires high bandwidth and low-latency communication in the uplink direction, as shown in Table 1. While it is of utmost importance that the camera information is uploaded reliably to the edge cloud, the output of the data-processing unit needs to be promptly transmitted to the LMD-w control unit to ensure the effective melting of the work piece in the downlink direction. The 5G system needs to support low and reliable latency to enable a timely sudden stop, slow-down of the process or power adjustment to guarantee the integrity and precision of workpieces. Moreover, the robot arm inside the MIRA cell features an interchangeable tool head (in red) allowing it to perform a variety of tasks. This increase in operational reliability and flexibility is enabled

through wireless technology facilitating seamless transition between different processes. Additionally, it helps prevent damage to sensitive cables during frequent tool head changes. It is noteworthy that besides the critical traffic in the uplink direction (image data from the camera) and downlink direction (control command for the LMD-w and robotic arm), there is background asynchronous traffic in both uplink and downlink directions as indicated in Table 1. Please note that the requirements may vary slightly depending on the specifics of the use case implementation.

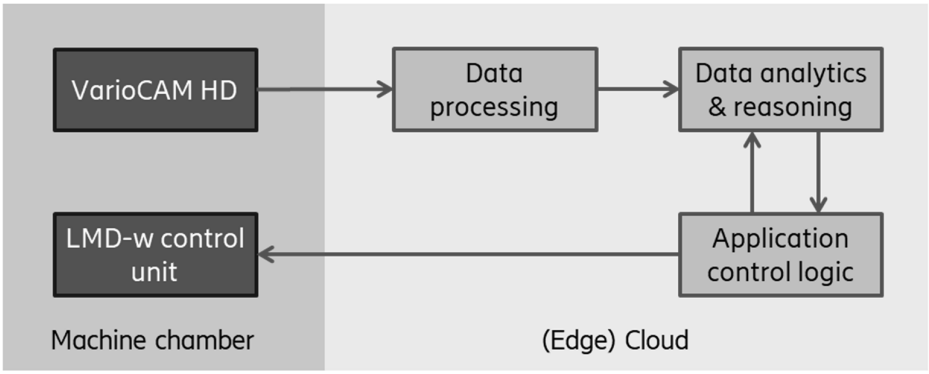


Figure 2. A simplified data-processing pipeline of the additive manufacturing use case.

Table 1. Additive manufacturing process and precision manufacturing robotics traffic flow configuration and communication requirements. Please note that the listed latency requirements are unidirectional and data size does not include the protocol overhead.

Use Case	Traffic Type	Traffic Direction	Traffic Periodicity	Data Size	Communication Requirements
Additive Manufacturing Process	Thermal camera	Uplink	5 ms	1000 B–50 kB	Latency < 10 ms Reliability > 99.9%
	Monitoring and status information	Uplink	Asynchronous	1000 B–8000 B	Latency < 100 ms Reliability > 90% (best effort)
	Edge-control commands	Downlink	8 ms–100 ms	18 B–500 B	Latency < 8 ms Reliability > 99.9%
	Software and configuration updates for camera module	Uplink	Asynchronous (occasional)	100 B–1400 B	Latency < 100 ms Reliability > 90% (best effort)
Precision Manufacturing Robotics	LiDAR data	Uplink	20 ms	160 B–1000 B	Latency < 40 ms Reliability > 99.99%
	Camera data	Uplink	100 ms	1000 B–5000 B	Latency < 40 ms Reliability > 99.99%
	Edge-control commands	Downlink	8 ms–10 ms	80 B	Latency < 40 ms Reliability > 99.99%

3.2. Precision Manufacturing Robotics

There is an increasing use of mobile robots on industrial shopfloors to allow for flexibility and enhance the accuracy, efficiency and reliability of precision manufacturing processes. Mobile robots can maneuver freely on an industrial shopfloor and perform a multitude of tasks at different locations. Equipped with advanced sensors and control systems, mobile robots can achieve high levels of precision for tasks such as assembly or quality inspection [31]. Industrial robots perform tasks such as micro-assembly or

component placement. These require reliably low-latency communication to make real-time adjustments of, e.g., the movement of the robot arm or the speed of the robot base [32]. The sensors collect data on various parameters, such as position, speed, orientation and environmental conditions. In this regard, mobile robots often rely on high-resolution sensors, such as LiDAR or cameras for navigation and mapping. These sensors require high data throughput to process and analyze the data in a (edge) processing unit as shown in Figure 3. For precision manufacturing robotics, mobile robots require real-time responsiveness. Path correction, dynamic interaction with objects, collaborative robot tasks or obstacle avoidance require low-latency communication.

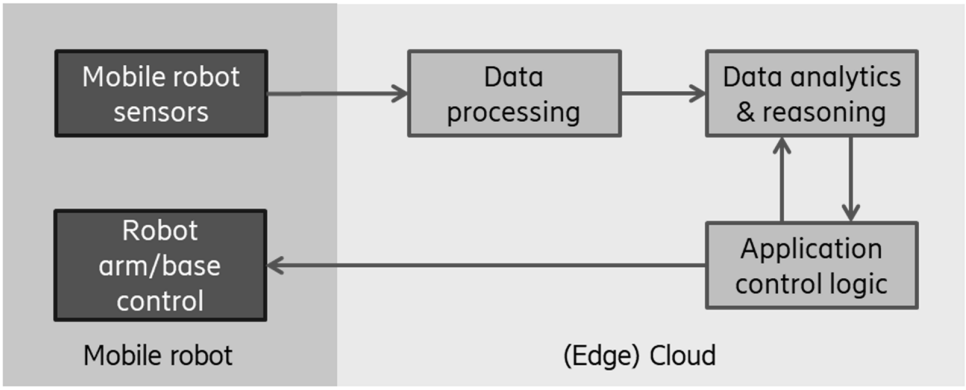


Figure 3. A simplified data-processing pipeline of the precision manufacturing robotic use case.

We investigate a mobile robotic use case for precision manufacturing and explore the potential benefits and challenges on the use of 5G mmW system for the communication requirements derived from our previous studies [8,31,32]. The robotics platform of the precision manufacturing use case is equipped with a LiDAR sensor and a camera transmitting information towards the edge application. The sensor data are processed and feedback commands to the robot are sent to adjust its position, orientation or speed, or the movement of its robot arm and base. The traffic profiles and requirements of the use case are presented in Table 1.

4. Experimental Setup and Methodology

In this section, we describe in detail the experimental setup and over-the-air testing methodology used for the evaluation of the 5G mmW system in a real production environment.

4.1. Experimental Setup

The performance evaluation of the commercial off-the-shelf (COTS) 5G mmW system has been carried out on the Fraunhofer IPT shopfloor in Aachen, Germany. The shopfloor covers an area of approximately 2700 m^2, featuring over 50 machines of various sizes, and serves as a representative example of a realistic large-scale indoor industrial environment. The 5G NPN deployment includes a 5G Non-Standalone (NSA) network, with an LTE anchor on band 7 (B7) alongside 5G NR mmW frequencies on bands n257 and n258. In 5G NSA deployments, the LTE and NR bands are used for signaling and data transmissions, respectively. In our paper, we evaluate the performance of the data transmissions, i.e., the 5G mmW frequency bands. The spectrum is licensed for private network deployments by the German spectrum regulatory authority, Bundesnetzagentur (BNetzA) [33]. The license provides 800 MHz of bandwidth allocation in the frequency range from 26.7 GHz to 27.5 GHz. In the experimental setup, the licensed bandwidth is divided into eight component carriers (CCs) of 100 MHz each. In 5G systems, particularly FR2 deployments, enhanced beamforming capabilities are crucial for overcoming propagation losses and

improving signal coverage and quality. The 5G NR cell on the Fraunhofer IPT shopfloor has vertical and horizontal analog beamforming configuration with +/− 60 degrees in azimuth and +/− 15 degrees in elevation, respectively. Further details on the 5G mmW network configuration can be found in Table 2. Unless stated otherwise, in UL transmission, we use a prescheduling scheme [34], where a UE keep receiving a grant upfront for data transmission without requiring a request for the grant explicitly as in the classical dynamic scheduling scheme. We use commercially available end devices in our measurement campaign. One device includes a Quectel RG530F-EU modem equipped with a Qualcomm Snapdragon x65 with FR2 support used for latency measurements. The Sony Xperia 1V with a Qualcomm Snapdragon x70 modem platform is used for throughput measurements.

Table 2. Configuration of 5G network and end devices in our experimental setup.

	Parameter	Description/Value
5G Network	Radio Unit	Ericsson AIR 1281
	Frequency band	5G NR n257, n258
	Duplexing scheme	Time Division Duplexing (TDD)
	Frequency range	26.7 to 27.5 GHz
	TDD pattern	DDDSU, DDSUU, DSUUU
	TDD special slot pattern (D:G:U)	10:2:2 (DDDSU), 12:2:2 (DDSUU and DSUUU)
	Component Carriers (CCs)	8
	Bandwidth per CC	100 MHz
	Subcarrier Spacing (SCS)	120 kHz
	Transmit power	2 W
5G End Devices	Device model	Quectel 5GDM01EK with Quectel RG530F-EU
	Chipset	Qualcomm SDX65
	FR2 MIMO capabilities	DL 2 × 2, UL 2 × 2
	Supported CCs	8 CCs DL, 4 CCs UL
	Device model	Sony Xperia 1V
	Chipset	Qualcomm SDX70
	FR2 MIMO capabilities	DL 4 × 4, UL 2 × 2
	Supported CCs	8 CCs DL, 4 CCs UL

The shopfloor at Fraunhofer IPT, as shown in Figure 4, is divided into two aisles where machines are distributed on the sides and in the middle of the shopfloor. The middle area is further divided around the center of the shopfloor with a corridor that crosses from one aisle to the other. On the shopfloor, the 5G mmW radio unit is positioned in one of the aisles at a height of approximately 5 m. This placement ensures a line of sight to the antenna, even from the opposite end of the aisle, at a distance of approximately 90 m. In our measurements, we consider different scenarios to assess the performance of the 5G mmWave system based on the deployment characteristics of the use cases as presented in Section 3. In particular, three different UE locations have been identified, ranging from close to far (labeled as 1, 2 and 3 in Figure 4) relative to the radio, allows us to analyze the performance of the 5G mmW system in different line-of-sight (LOS) conditions. Due to the height of the antenna and the presence of machines, there is no direct line of sight (NLOS) to the 5G radio on the other aisle. Similarly, we identify three locations (labeled as 4, 5 and 6 in Figure 4) to evaluate the 5G mmW system performance at positions near, midway and far from the antenna. We also evaluate the performance of the 5G system when the UE is placed inside a closed machine chamber (MIRA Cell) to realistically investigate the performance of the 5G mmW system for thermal camera use cases. At location (7), the 5G terminal device is in an obstructed line of sight (OLOS) with the 5G base station radio

unit. In our analysis, we fix the orientation of the device throughout all the experimental scenarios. In LOS, the device antennas are aligned to the radio unit antennas. In NLOS locations, the device orientation is maintained such that the device antennas face the end of the hall where the radio unit is located, but they do not directly point to the radio unit itself. At OLOS, the device is facing the gas-filled double glass window of the laser robot machine chamber as shown in Figure 4.

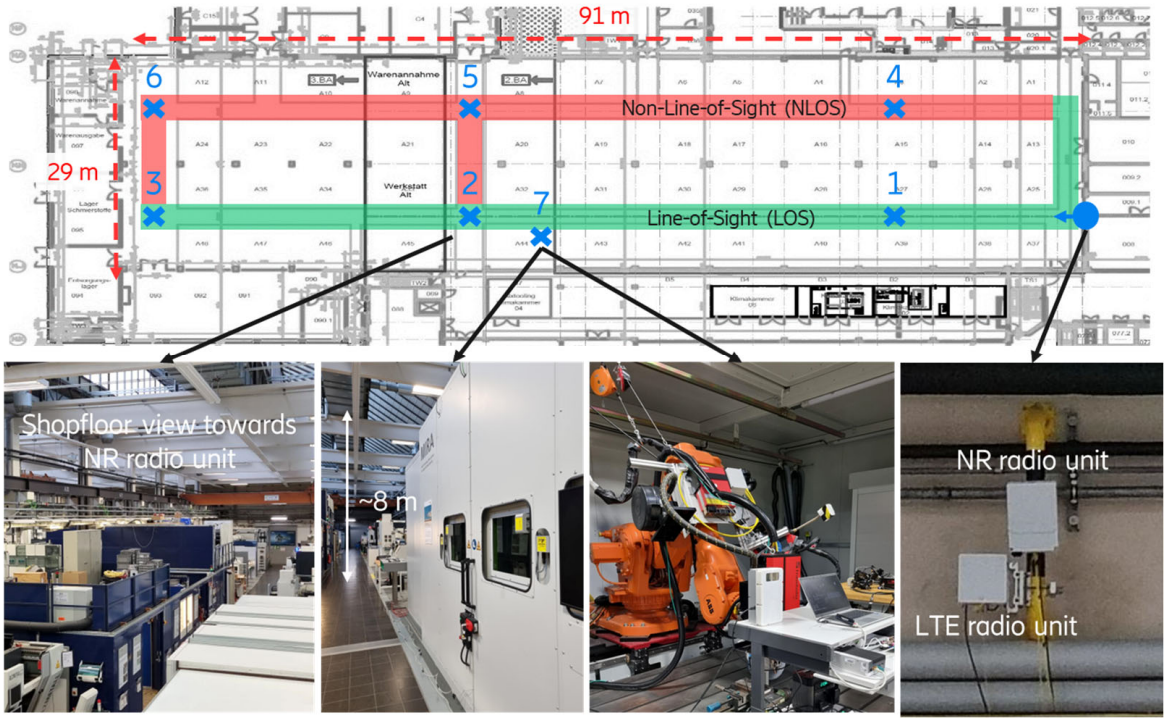


Figure 4. Shopfloor layout and various snapshots at Fraunhofer IPT with marked locations of the test device in both line of sight and non-line of sight with the radio units. The experimental setup (bottom, third picture from left) is shown at location 7 inside the machine chamber for the additive manufacturing use case. The symbol "x" indicates the position of the device at different locations.

We explore another common use-case scenario from precision manufacturing robotics, e.g., when a mobile robot navigates around on the shopfloor or when a workpiece moves between different automation cells in an assembly line. To mimic this scenario, we use a moveable trolley setup and move it between different test locations. Our focus has been on the performance characteristics with a transition from a LOS to a NLOS position, and vice versa. We further explore the 5G system performance for different configuration parameters, such as the TDD frame structure and the level of link robustness.

4.2. Experimental Methodology

In this section, we describe our experimental methodology for evaluating the one-way uplink and downlink performance of the 5G system with a focus on three main KPIs: latency, reliability and throughput. The requirements of industrial applications often demand low latency for real-time control and monitoring, high reliability to ensure consistent and safe operations and high throughput to support data-intensive processes and maintain seamless connectivity for a large number of devices across the industrial shopfloor.

In the 5G FR2 bands, only Time Division Duplexing (TDD) deployments are supported. The TDD deployments are particularly relevant for 5G private networks, especially indoors, as these allow tailoring resource allocation in uplink and downlink directions, according to the enterprise application requirement. We study three different TDD frame structures with

different configurations of the downlink (D), uplink (U) and special (S) slots. One of the investigated TDD pattern allocates more resources to downlink transmissions (DDDSU), another balances the number of D and U slots (DDSUU) and the third pattern allocates more resources to uplink transmissions (DSUUU). D and U slots can carry control information and data traffic for downlink and uplink, respectively. S slots consist of symbols mainly used for downlink transmissions (control and data) and some uplink transmissions (control), while also serving as guard (G) during the transition between the D and U slots.

Considering the use cases as described in Section 3, we carry out one-way traffic for performance evaluation instead of two-way performance measurements with strict cycles of uplink and downlink traffic having the same data size. Moreover, the 5G performance in uplink and downlink directions can be different from each other owing to the differences in the transmission and reception capabilities of terminal devices and base stations such as the transmit power levels, MIMO scheme, available bandwidth resources, protocol signaling overhead and the processing power [35]. In this context, a field-programmable gate array (FPGA)-based tool is used to generate one-way traffic. The FPGA-based tool allows us to emulate industrial traffic profiles and accurately measure one-way latency and throughput. The FPGA-based tool can be used to generate configurable automation traffic profiles. In order to avoid precise time synchronization between the sender and receiver for accurate timing measurements, the same FPGA board is used as the data sink for the 5G UE or the 5G Network to carry out timestamping from the coherent sub-microsecond clock on the FPGA board. In our evaluation, the traffic between the automation field device (i.e., sensors, robots, machines) and the cloud-based controller can be emulated. The FPGA-based tool connects to a 5G mmW UE and the N6 interface of the 5G mmW network as illustrated in Figure 5. Please note that the one-way latency represents the end-to-end delay including device processing times, propagation and transmission latency, 5G radio, baseband unit and core network processing times.

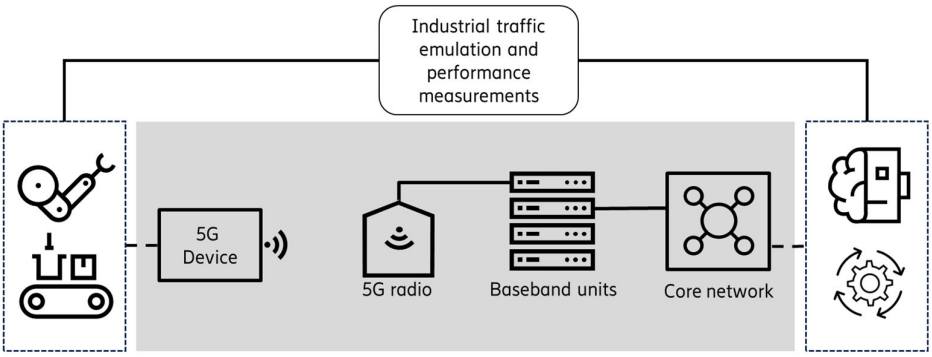


Figure 5. Schematics of the experimental setup used for emulating industrial traffic and carrying out performance measurements.

We collected at least 100,000 measurement samples for each experimental scenario to ensure that our results are statistically significant. To evaluate the statistical significance of the data we calculate Student's *t*-distribution. We obtain the confidence intervals of multiple statistical values (e.g., mean, median, 90th percentile, etc.) of 5 equally sized batches from each time-series experiment. The overall empirical data collection and measurement campaign required several days of measurement time. Alongside the throughput and latency measurements, network tracing information is collected based on a tool developed to gather 5G network insights during the experiments. The tool allows access to network information from various nodes, including the Radio Access Network (RAN), Core Network and Transport Network. A granularity of one second is used for gathering the aggregated

network state and baseband tracing information to capture dynamic network behavior and monitor 5G mmW performance behavior in an online fashion.

5. Performance Evaluation in an Industrial Environment

Uplink and downlink throughput and latency measurements were performed in the 5G mmW system with traffic characteristics applicable for the investigated industrial use cases based on the methodology described in Section 4.

5.1. One-Way Latency Evaluation

The initial results include DL and UL latency for a deployment scenario at Position 2, as shown in Figure 4, with direct LOS and the DDSUU TDD frame structure. At this location, the radio propagation conditions are expected to be very favorable as the static device has a direct LOS to the NR radio unit. The sample set collected for the UL and DL latency indicates a bounded latency of less than 10 ms, as shown in Figure 6. The minimum latency values are observed to be around 1 ms and 1.8 ms for DL and UL transmissions, respectively. The mean latencies of the experiment are 1.46 ms (DL) and 2.22 ms (UL). Theoretically, if no processing delays are accounted, then the minimum DL delay should be 0.125 ms (one TDD slot duration for 120 kHz SCS) for a packet received right before a downlink slot. In this regard, our tools and measurement setup lack the capability to determine the origin of the extra delays. Generally, those are caused by processing delays of the 5G UE, radio, baseband unit and core.

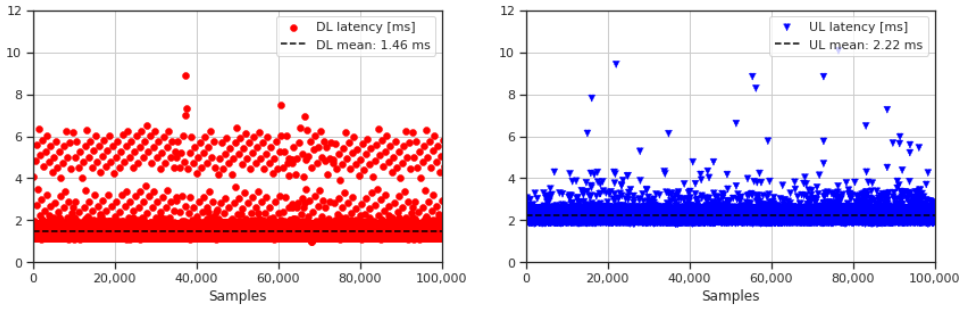


Figure 6. DL (**left**) and UL (**right**) latency time series at Position 2 with TDD pattern DDSUU.

Nevertheless, the time-series results indicate a larger number of peaks in the DL. Therefore, we present the complementary cumulative distribution function (CCDF) to statistically evaluate the latency distribution in UL and DL. As the reliability requirements in industrial use cases often indicate the necessary latency bounds for high percentiles, the CCDF is presented in a logarithmic scale in Figure 7 (left). While the latency distributions in UL and DL behave similarly slightly beyond the 10^{-2} percentile (99th percentile), a tail effect can be observed before the 10^{-3} percentile (99.9th percentile). The result indicates that the peaks observed in the time-series distribution represent less than 1% of the sample set. Nevertheless, the differences in the high percentiles between the UL and DL distribution are explained by the moderately large number of retransmissions. Based on the network logs we observe lower selected UL modulation and coding scheme (MCS) values compared to DL, leading to more robust transmissions. Furthermore, in our experimental setup, the maximum configured modulation is 256 QAM and 64 QAM for DL and UL, respectively. Moreover, it can be observed that the peaks above 4 ms and 6 ms represent less than 0.1% of the sample set for UL and DL, respectively. Additionally, we evaluate the confidence intervals of the sample set based on Student's *t*-distribution for different percentiles in Figure 7 (right). The sample set of each experiment is equally divided into five smaller sample sets. The confidence intervals are obtained based on statistical percentiles (50th, 90th, 99th and 99.9th percentile) of the small sample sets under evaluation for each of

the experiments. The highest percentage difference in the confidence interval can be observed for the 99.9th percentile in DL. For this value, the confidence interval is 4.3% with lower and upper limits of 5.31 ms and 5.79 ms, respectively. The rest of the values have a confidence interval of around 1% or lower. Similar results are obtained for all the sample sets presented in the paper. Therefore, based on the confidence interval results, we determine that our sample set of 100,000 samples is sufficient to reliably estimate values up to the 99.9th percentile.

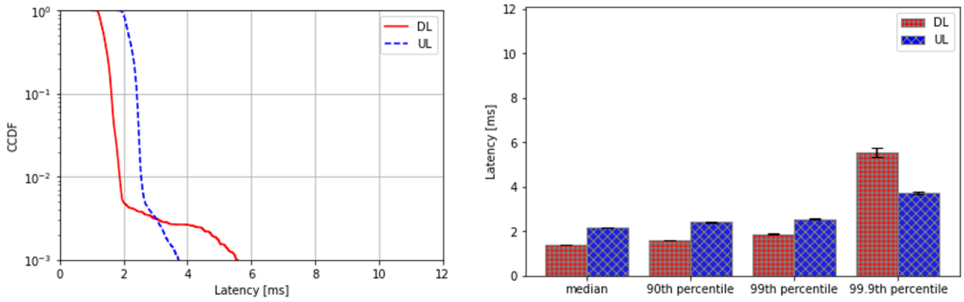


Figure 7. UL and DL latency CCDF (**left**) and bar graphs (**right**) of selected percentiles with confidence intervals.

In the following performance evaluation subsections, we present the latency bar graphs for different percentiles for simplicity. The higher percentiles highlight the latency bounds that are critical for ensuring the mission-critical communication requirements of industrial applications. These bounds help in understanding the latency performance, which is essential for ensuring that time-sensitive operations are executed reliably.

5.2. Comparative Analysis of Different TDD Frame Structures

In this subsection, we study the throughput and latency performance at Position 2 as shown in Figure 4 for different TDD frame structures. The device (Sony Xperia 1V) is placed vertically facing the 5G radio with a direct LOS. At this location, the measured downlink (DL) throughput is observed to be up to 3.98 Gbps, 2.94 Gbps and 2.15 Gbps for DDDSU, DDSUU and DSUUU with eight CCs, respectively. One may clearly observe that the higher the number of DL slots, the higher the achieved DL throughput is. Similarly, the uplink (UL) throughput for DDDSU, DDSUU and DSUUU is observed to be up to 923 Mbps, 1390 Mbps and 2120 Mbps, respectively. The results indicate an increasing throughput for UL with an increasing number of UL slots, and vice versa. While the throughput for both DL and UL is generally high, the overall UL throughput is constrained by the UE configuration support of a maximum of four CCs unlike DL, where all eight available CCs can be utilized. Furthermore, the maximum configured modulation for DL allows the transport of larger over-the-air transmissions compared to UL.

At the same location, the unidirectional UL and DL latency are independently measured for the aforementioned TDD patterns. The traffic profile selected involves transmitting a 1000-byte payload at periodic intervals. This approach enables us to systematically evaluate the 5G system latency characteristics and understand its behavior for the traffic profiles of the industrial use cases.

In Figure 8, four statistical values (median, 90th, 99th and 99.9th percentiles) are studied for each TDD pattern. In this regard, Figure 8 (left) highlights that the DL latency bound of the 5G mmW system at the 99.9th percentile is below 5.85 ms, independent of the TDD pattern under LOS conditions. The DL latency at the 90th percentile with a latency bound of 1.52, 1.62 and 1.85 ms for each of the investigated TDD patterns. In Figure 8 (right), the UL has been observed to be 3.84 ms for all the TDD patterns evaluated at the 99.9th percentile. From the UL baseband traces, we observe that the selected UL modulation

coding scheme (MCS) is generally more robust compared to DL, causing a smaller number of retransmissions and thereby resulting in lower latency behavior. Please note that the configured BLER target in the experiments is 10%. At the same time, we can observe that in UL, DSUUU maintains a stable performance compared to other TDD patterns at 99th and 99.9th percentile values. The TDD patterns with more UL slots allow for a better UL channel estimation (with more UL signals for performing channel estimation), which leads to fewer retransmissions and a higher reliability, as can be observed at higher latency percentiles. The network traces reveal that the selected UL MCS for DDDSU and DDSUU is occasionally higher compared to DSUUU, which leads to more packet retransmissions. In this regard, our results indicate that the performance of the 5G mmW system in LOS conditions outperforms the typical network KPIs of the 5G sub-7 GHz deployments.

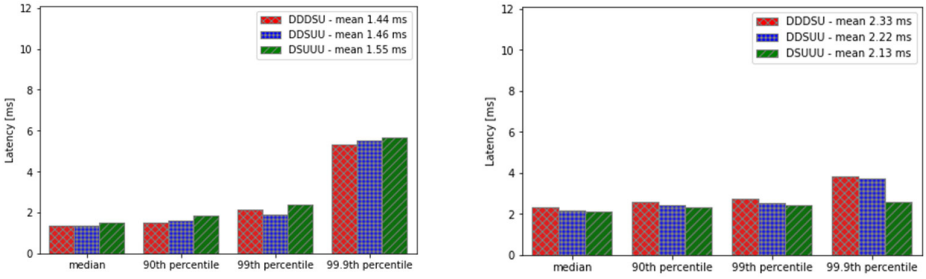


Figure 8. DL (**left**) and UL (**right**) latency of the 5G mmW system for different TDD frame structures.

5.3. Analysis of LOS, NLOS and OLOS Scenarios

We evaluate the performance of the 5G mmW system when a static device is located at different locations on the shopfloor, as illustrated in Figure 4. In this analysis, we present the results for the TDD pattern, DDSUU. From the network traces, we observe that the synchronization signal block (SSB) reference signal received power (RSRP) decreases as (i) we move far away from the radio unit and (ii) under NLOS conditions as shown in Table 3. The DL beam index also indicates the spatial distribution of the beams for the different device positions on the shopfloor.

Table 3. Observed radio signal power levels (SSB RSRP) and beam index information at different locations.

Position ID	Position	SSB RSRP	DL Beam Index
1	LOS-near	−62.50 dBm	10
2	LOS-mid	−69.85 dBm	10
3	LOS-far	−74.50 dBm	10
4	NLOS-near	−86.50 dBm	8
5	NLOS-mid	−92.63 dBm	11
6	NLOS-far	−98.10 dBm	7
7	OLOS	−100.32 dBm	10

We observe that the UL latency behavior of the 5G mmW system remains similar at different positions independent of the distance from the base station and the radio propagation conditions as shown in Figure 9 (left). The results indicate that, for the most challenging radio conditions (NLOS-far and OLOS) investigated in this paper, the 5G system is capable of ensuring low-UL-latency bounds with high reliability (below 4 ms at 99.9th percentile). In DL, the latency under NLOS conditions, when the device is near the base station, remains comparable to scenarios where the device antennas maintain LOS with the 5G mmW base station antenna as shown in Figure 9 (right). However, as the device moves to a faraway scenario, the median values increase in NLOS conditions. This increased delay is caused by the challenging radio conditions. Similar latency performance

at the median and 90th percentile can be observed when the device is placed in a machine chamber under OLOS conditions. At this location, the device is closed in a machine chamber with some windows (as shown in Figure 4) causing similar effects as when the device is far away in NLOS conditions. Compared to the UL, the DL results indicate that the device suffers in challenging radio conditions. While advanced, the device antenna receivers suffer in mitigating the effects of multipath propagation in mmW deployments. As a result, this can contribute to increased latency in the DL.

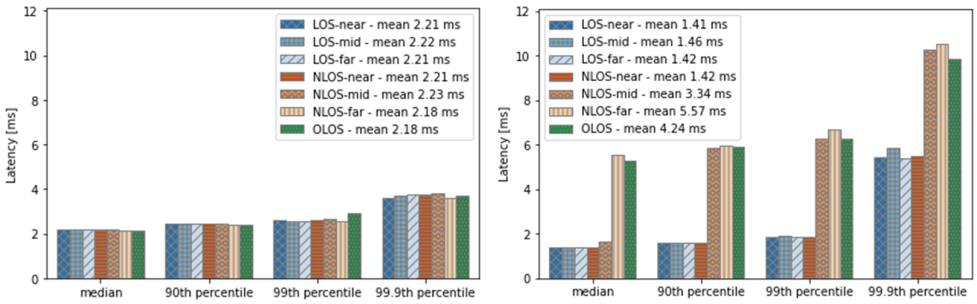


Figure 9. UL (**left**) and DL (**right**) latency of the 5G mmW system for different locations with LOS, NLOS and OLOS scenarios.

5.4. Evaluation of Mobile and Static Devices

It is believed that mmW transmissions suit static deployments; we also investigate the performance of the 5G mmW system and, in particular, the beam-switching and beam-steering schemes when a UE is moving between positions with LOS and NLOS coverage. As an example, in Figure 10, we analyze the performance of a moving device from positions 2 to 5 and vice versa. In both figures, it can be observed that the latency performance differs when the device moves from a LOS to a NLOS location. While the impact is more visible in DL, the same effect can be observed in UL. Due to the changing channel conditions, the 5G mmW system accordingly applies to a more robust or optimistic MCS selection. As a more optimistic (higher value) MCS in LOS conditions tend to carry larger data portions over the air, the transport block must be divided in smaller data transmissions for some NLOS scenarios due to more robust (lower value) MCS selection. The result highlights the performance of the 5G system, especially in UL, as we observe notable performance in UL for NLOS conditions independent of whether the device is static or mobile. Therefore, emphasizing the receiver capabilities of the 5G mmW base station. Particularly, when the device moves from a LOS to a NLOS position high peaks appear in the latency performance. Those can be caused due to the shadowing effects, multipath interference and challenges maintaining beam alignment.

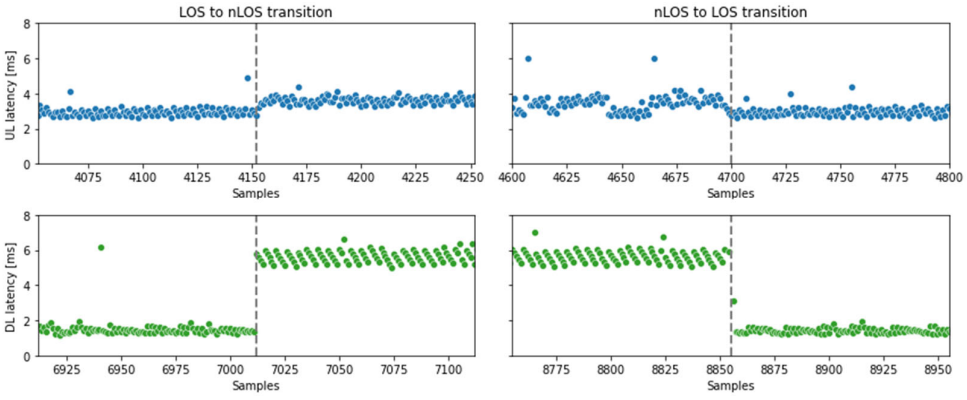


Figure 10. Zoomed-in portion of the UL and DL latency for static and moving UEs showing transitions from LOS to NLOS (**left**) and NLOS to LOS (**right**) scenarios.

5.5. Performance Assessment of Link Robustness Configurations

We analyze the performance of the 5G mmW system for different levels of link robustness, which is achieved through the configuration of different block error rate (BLER) targets. While the previous experiments are carried out by using a typical BLER target value of 10%, we further study the performance of the BLER targets of 1 and 0.1%. The BLER target is used in 5G systems to offset the value of the signal-to-interference-plus-noise ratio (SINR) estimation based on the channel feedback at the medium access control (MAC) layer. A lower BLER target could generate higher offsets when the feedback carries non-acknowledgements (retransmissions needed). Effectively, the SINR utilized for the assignment of the MCS is lower leading to more robust transmissions. Please note that the MCS index has an integer value from 0 to 31 with the highest robustness for MCS 0. The selection of MCS values also determines the overall throughput of the system, higher MCS values enable greater data rates and vice versa. In our experimental setup, we study the effects of different link robustness levels when a device is located at LOS (Position 2 as in Figure 4) and NLOS (Position 5 as in Figure 4) conditions. In Table 4, the UL and DL throughput values for the different BLER targets are shown. We can observe in the throughput results that it is primarily limited by the radio propagation conditions while the BLER change impact is not that significant. In LOS conditions, the probability of retransmission is low and, therefore, the selected MCS remains similar at different locations. A similar throughput impact has been observed in NLOS conditions in both test locations. As for LOS conditions, the baseband logs indicate a very low number of retransmissions in NLOS. However, the MCS for UL and DL is anyway selected to be robust in order to cope with the challenging channel conditions, and hence, the relative impact of different NLOS locations is less pronounced.

Table 4. Throughput and average MCS values for different BLER targets at LOS and NLOS radio propagation conditions.

ID	Position	BLER Target	DL Thp.	Avg. DL MCS	UL Thp.	Avg. UL MCS
2	LOS-mid	10%	2940 Mbps	23.15	1078 Mbps	18.24
2	LOS-mid	1%	2362 Mbps	21.01	1014 Mbps	17.88
2	LOS-mid	0.1%	2439 Mbps	22.66	884 Mbps	16.29
5	NLOS-mid	10%	1140 Mbps	18.41	91 Mbps	10.94
5	NLOS-mid	1%	1200 Mbps	17.98	88 Mbps	11.15
5	NLOS-mid	0.1%	962 Mbps	17.04	86 Mbps	11.85

In Figure 11, the UL and DL latency performances demonstrate that the previously discussed 5G mmW performance is not dominated by the effects of the retransmissions. It can be observed that at the NLOS where more retransmissions can be expected due to more challenging radio conditions, the performance for 0.1% BLER target is similar to the performance of 10% at the different percentiles.

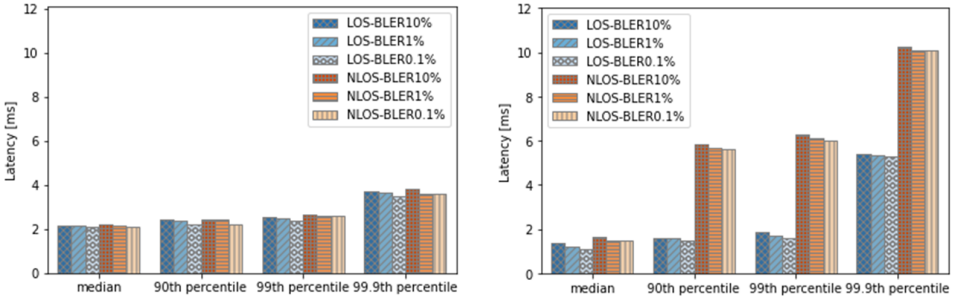


Figure 11. UL (**left**) and DL (**right**) latency of the 5G mmW system for different link robustness (BLER target) configurations in LOS and NLOS conditions.

6. Conclusions and Future Work

In this paper, we presented our over-the-air empirical performance results on the use of the 5G mmW system for industrial use cases in a real production environment. In the literature, 5G non-public-network deployments for industrial applications have mainly been limited to the FR1 or sub-7 GHz bands. The sub-7 GHz spectrum, albeit having good signal propagation characteristics, has limited available bandwidth for 5G non-public industrial networks. It is generally assumed that mmW transmissions significantly suffer from signal propagation issues and, therefore, performance guarantees with mmW wireless networks are hard to achieve especially for mission-critical industrial applications. Our detailed experimental results in terms of latency, reliability aspects and throughput indicate that the 5G mmW system can effectively address the communication requirements of several industrial static and low-mobility use cases. In LOS scenarios, the 5G FR2 system performance outperforms typical values of 5G FR1 deployments. While the LOS coverage for the 5G mmW transmissions is very good, industrial environments with typically lots of metallic and other reflective surfaces also allow for decent NLOS coverage. Our experimental results for various deployment positions with LOS and NLOS scenarios indicate that 5G mmW system shows latency of ca. 4 ms and ca. 10 ms with the 99.9th percentile for UL and DL transmissions, respectively. The UL performance for the 99.9th percentile leverages better decoding capability at the base station, especially in NLOS scenarios with lower signal levels. The large available bandwidth in 5G mmW bands allows us to achieve multi-Gbps throughput in uplink and downlink directions, which can address the demands of data rate-intensive industrial applications and scalable deployments. We also explored the effect of 5G system configuration parameters such as the TDD pattern and the BLER target and provided insights into the 5G mmW system behavior based on the baseband tracing information. Our results indicate different performances in industrial environments of LOS and NLOS scenarios in both static and mobile settings. This suggests that multi-cell deployments may be necessary to ensure comprehensive coverage across all areas on an industrial shopfloor. While we considered only a single 5G mmW cell deployment in this paper, as part of our ongoing and future work, we are empirically investigating the performance behavior due to multiple coexisting 5G mmW cells in industrial environments.

Author Contributions: Conceptualization and validation, J.B.C. and J.A.; methodology, software development and research, J.B.C., J.A., B.-E.O. and N.B.; writing and formal analysis, J.B.C., J.A., B.-E.O., N.B., N.K., R.H.S., F.P. and D.S.-M. All authors have read and agreed to the published version of the manuscript.

Funding: This research was funded by the EU project TARGET-X. The TARGET-X project has received funding from the Smart Networks and Services Joint Undertaking (SNS JU) under the European Union's Horizon Europe research and innovation program under Grant Agreement No: 101096614.

Data Availability Statement: Data are contained within the article.

Conflicts of Interest: Authors Jordi Biosca Caro, Junaid Ansari, Bengt-Erik Olsson, Falko Popp and Daniel Scheike-Momberg are employed by companies Ericsson GmbH, Ericsson AB and Qualcomm, respectively. The remaining authors declare that the research was conducted in the absence of any commercial or financial relationships that could be construed as a potential conflict of interest.

References

1. 5G-ACIA Whitepaper on 5G for Industrial Internet of Things (IIoT): Capabilities, Features, and Potential. Available online: https://5g-acia.org/download/18767/?version=A4 (accessed on 19 October 2024).
2. Malekzadeh, M. Performance prediction and enhancement of 5G networks based on linear regression machine learning. *J. Wirel. Com. Netw.* **2023**, *2023*, 74. [CrossRef]
3. Hamidi-Sepehr, F.; Sajadieh, M.; Panteleev, S.; Islam, T.; Karls, I.; Chatterjee, D.; Ansari, J. 5G URLLC: Evolution of High-Performance Wireless Networking for Industrial Automation. *IEEE Commun. Stand. Mag.* **2021**, *5*, 132–140. [CrossRef]
4. Rappaport, T.S.; Heath, R.W., Jr.; Daniels, R.C.; Murdock, J.N. *Millimeter Wave Wireless Communications*; Pearson Education: London, UK, 2015.
5. Lackner, T.; Hermann, J.; Dietrich, F.; Kuhn, C.; Angos-Mediavilla, M.; Jooste, W.; Palm, D. Measurement and comparison of data rate and time delay of end-devices in licensed sub-6 GHz 5G standalone non-public networks. *Procedia CIRP* **2022**, *107*, 1132–1137. [CrossRef]
6. Majed, M.B.; Rahman, T.A.; Abdul Aziz, O. Propagation Path Loss Modeling and Outdoor Coverage Measurements Review in Millimeter Wave Bands for 5G Cellular Communications. *Int. J. Electr. Comput. Eng.* **2018**, *8*, 2254. [CrossRef]
7. 3GPP Technical Specifications TS 22.261. Available online: https://www.etsi.org/deliver/etsi_ts/122200_122299/122261/16.14.00_60/ts_122261v161400p.pdf (accessed on 18 December 2024).
8. Ansari, J.; Hsiao, T.S.; Jafari, M.H.; Varga, B.; Farkas, J.; Moldován, I.; Göppert, A.; Schmitt, R.H. 5G enabled flexible lineless assembly systems with edge cloud controlled mobile robots. In Proceedings of the IEEE 33rd Annual International Symposium on Personal, Indoor and Mobile Radio Communications, Kyoto, Japan, 12–15 September 2022.
9. Fraunhofer Institute for Production Technology, Aachen Germany. Available online: https://www.ipt.fraunhofer.de/ (accessed on 19 October 2024).
10. 3GPP Service Requirements for Cyber-Physical Control Applications in Vertical Domains. Technical Specification TS 22.104 V18.1.0. 2021. Available online: https://www.etsi.org/deliver/etsi_ts/122100_122199/122104/16.05.00_60/ts_122104v160500p.pdf (accessed on 19 October 2024).
11. 5G-ACIA White paper, Key 5G Use Cases and Requirements. 2020. Available online: https://5g-acia.org/download/18727/?tmstv=1706108588 (accessed on 19 October 2024).
12. Gharibvand, V.; Kolamroudi, M.K.; Zeeshan, Q.; Çınar, Z.M.; Sahmani, S.; Asmael, M.; Safaei, B. Cloud based manufacturing: A review of recent developments in architectures, technologies, infrastructures, platforms and associated challenges. *Int. J. Adv. Manuf. Technol.* **2024**, *131*, 93–123. [CrossRef]
13. Rischke, J.; Sossalla, P.; Itting, S.; Fitzek, F.H.P.; Reisslein, M. 5G Campus Networks: A First Measurement Study. *IEEE Access* **2021**, *9*, 121786–121803. [CrossRef]
14. Xu, D.; Zhou, A.; Zhang, X.; Wang, X.; Liu, X.; An, C.; Shi, Y.; Liu, L.; Ma, H. Understanding Operational 5G: A First Measurement Study on Its Coverage, Performance and Energy Consumption. In Proceedings of the Annual Conference of the ACM Special Interest Group on Data Communication on the Applications, Technologies, Architectures, and Protocols for Computer Communication, New York, NY, USA, 10–14 August 2020.
15. Next Generation Mobile Networks (NGMN) Alliance White Paper on 5G TDD Uplink. 2021. Available online: https://www.ngmn.org/wp-content/uploads/220117-5G-TDD-Uplink-White-Paper-v1.0.pdf (accessed on 19 October 2024).
16. Yang, G. Throughput and Latency of Millimeter-Wave Networks: Performance Analyses and Design Principles. Ph.D. Thesis, KTH Royal Institute of Technology, Stockholm, Sweden, 2018.
17. Al-Saman, A.; Cheffena, M.; Elijah, O.; Al-Gumaei, Y.A.; Abdul Rahim, S.K.; Al-Hadhrami, T. Survey of Millimeter-Wave Propagation Measurements and Models in Indoor Environments. *Electronics* **2021**, *10*, 1653. [CrossRef]
18. Wang, X.; Kong, L.; Kong, F.; Qiu, F.; Xia, M.; Arnon, S.; Chen, G. Millimeter Wave Communication: A Comprehensive Survey. *IEEE Commun. Surv. Tutor.* **2018**, *20*, 1616–1653. [CrossRef]
19. Inoue, Y.; Kishiyama, Y.; Suyama, S.; Kepler, J.; Cudak, M.; Okumura, Y. Field Experiments on 5G mmW Radio Access with Beam Tracking in Small Cell Environments. In Proceedings of the IEEE Globecom Workshops, San Diego, CA, USA, 6–10 December 2015.
20. Ansari, J.; Perpinias, N.; Nähring, A.; Mähönen, P.; Petrova, M. Empirical characterization of mm-wave communication links in realistic indoor scenarios. In Proceedings of the IEEE Wireless Communications and Networking Conference, New Orleans, LA, USA, 9–12 March 2015.

21. Raghavan, V.; Partyka, A.; Sampath, A.; Subramanian, S.; Koymen, O.H.; Ravid, K.; Cezanne, J.; Mukkavilli, K.; Li, J. Millimeter-Wave MIMO Prototype: Measurements and Experimental Results. *IEEE Commun. Mag.* **2018**, *56*, 202–209. [CrossRef]
22. Ghoshal, M.; Kong, Z.J.; Xu, Q.; Lu, Z.; Aggarwal, S.; Khan, I.; Li, Y.; Hu, Y.C.; Koutsonikolas, D. An in-depth study of uplink performance of 5G mmWave networks. In Proceedings of the ACM SIGCOMM Workshop on 5G and Beyond Network Measurements, Modeling, and Use Cases, Amsterdam, The Netherlands, 22 August 2022; pp. 29–35.
23. Zheng, K.; Wang, D.; Han, Y.; Zhao, X.; Wang, D. Performance and Measurement Analysis of a Commercial 5G Millimeter-Wave Network. *IEEE Access* **2020**, *8*, 163996–164011. [CrossRef]
24. Agubor, C.K.; Akwukwuegbu, I.; Olubiwe, M.; Nosiri, C.O.; Ehinomen, A.; Olukunle, A.A.; Okozi, S.O.; Ezema, L.; Okeke, B.C. A Comprehensive Review on the Feasibility and Challenges of Millimeter Wave in Emerging 5G Mobile Communication. *J. Adv. Sci. Technol. Eng. Syst.* **2019**, *4*, 138–144. [CrossRef]
25. Danger, M.; Arendt, C.; Schippers, H.; Böcker, S.; Muehleisen, M.; Becker, P.; Caro, J.B.; Gjorgjievska, G.; Latif, M.A.; Ansari, J.; et al. Performance Evaluation of IRS-Enhanced mmWave Connectivity for 6G Industrial Networks. In Proceedings of the IEEE International Symposium on Measurements & Networking (M&N), Rome, Italy, 2–5 July 2024.
26. Khan, M.F.; Raza, A.; Iqbal, A.; Rashid, A.; Jamshed, M.A.; Pesch, D. Performance Analysis of Intelligent Reflecting Surfaces for 5G/6G-Enabled Future Smart Industries with a Focus on Millimeter-Wave Band Communications. In Proceedings of the IEEE International Conference on Communications Workshops, Denver, CO, USA, 9–13 June 2024.
27. Ayadurai, V.; Narayanan, R.; Olsson, B.-E. Experiments with industrial robotics systems over an indoor 5G-NSA mmWave deployment. In Proceedings of the Joint European Conference on Networks and Communications & 6G Summit, Gothenburg, Sweden, 6–9 June 2023.
28. *ISO/ASTM 52900:2021*; Additive Manufacturing—General Principles—Fundamentals and Vocabulary. German version EN ISO/ASTM 52900:2021; ISO: Geneva, Switzerland, 2022.
29. Fraunhofer, I.P.T. Multi-Technology Platform. Available online: https://www.ipt.fraunhofer.de/en/offer/special-machines/multi-technology-platform.html (accessed on 19 October 2024).
30. Rupp, D.; Kuhlen, T.W.; Rarbach, S.; Wiechel, D.; Pottebaum, J.; Weidemann, T.; Tranh Tran, D.; Day, R.; Zielinski, J.; Koenig, V.; et al. Virtual Reality as a Tool for Monitoring Additive Manufacturing Processes via Digital Shadows. In Proceedings of the the VR/AR Workshop, Hamburg, Germany, 17–18 September 2024; Gesellschaft für Informatik e.V.: Berlin, Germany, 2024. [CrossRef]
31. Kehl, P.; Ansari, J.; Jafari, M.H.; Becker, P.; Sachs, J.; König, N.; Göppert, A.; Schmitt, R.H. Prototype of 5G Integrated with TSN for Edge-Controlled Mobile Robotics. *Electronics* **2022**, *11*, 1666. [CrossRef]
32. 5G-SMART Project Report on the Validation of 5G Use Cases in a Factory. Available online: https://5gsmart.eu/wp-content/uploads/5G-SMART-D4.4-v1.0.pdf (accessed on 19 October 2024).
33. BNetzA. Administrative Rules for Spectrum Assignments for Local Spectrum Usages in the 3700–3800 MHz Band. Available online: https://www.bundesnetzagentur.de/SharedDocs/Downloads/EN/Areas/Telecommunications/Companies/TelecomRegulation/FrequencyManagement/FrequencyAssignment/LocalBroadband3,7GHz.pdf?__blob=publicationFile&v=1 (accessed on 19 October 2024).
34. Ericsson Blog. A Technical Overview of Time-Critical Communication with 5G NR. 2021. Available online: https://www.ericsson.com/en/blog/2021/2/time-critical-communication--5g-nr (accessed on 19 December 2024).
35. Lucas-Estañ, M.C.; Coll-Perales, B.; Shimizu, T.; Gozalvez, J.; Higuchi, T.; Avedisov, S.; Altintas, O.; Sepulcre, M. An Analytical Latency Model and Evaluation of the Capacity of 5G NR to Support V2X Services using V2N2V Communications. *IEEE Trans. Veh. Technol.* **2023**, *72*, 2293–2306. [CrossRef]

Disclaimer/Publisher's Note: The statements, opinions and data contained in all publications are solely those of the individual author(s) and contributor(s) and not of MDPI and/or the editor(s). MDPI and/or the editor(s) disclaim responsibility for any injury to people or property resulting from any ideas, methods, instructions or products referred to in the content.